 doi:10.20944/preprints202107.0553.v1

Article

Novel cytological model for the identification of early oral cancer diagnostic markers: the carcinoma sequence model

Masami Kawaharada[1,2], Manabu Yamazaki[2], Satoshi Maruyama[3], Tatsuya Abé[2], Nyein Nyein Chan[1,2], Taiichi Kitano[3], Tadaharu Kobayashi[1], Takeyasu Maeda[4], Jun-ichi Tanuma[2,*]

[1] Division of Reconstructive Surgery for Oral and Maxillofacial Region, Faculty of Dentistry & Graduate School of Medical and Dental Sciences, Niigata University, Niigata 951-8514, Japan; kawaharada@dent.niigata-u.ac.jp (M.K.); nnchan@dent.niigata-u.ac.jp (N.N.C.); tadaharu@dent.niigata-u.ac.jp (T.K.)
[2] Division of Oral Pathology, Faculty of Dentistry & Graduate School of Medical and Dental Science, Niigata University, Niigata 951-8514, Japan; manabu@dent.niigata-u.ac.jp (M.Y.); abet@dent.niigata-u.ac.jp (T.A.)
[3] Oral Pathology Section, Department of Surgical Pathology, Niigata University Medical and Dental Hospital, Niigata 951-8520, Japan; maru@dent.niigata-u.ac.jp (S.M.); kitano-t@dent.niigata-u.ac.jp (T.K.)
[4] Division of Oral Anatomy, Faculty of Dentistry and Graduate School of Medical and Dental Sciences, Niigata University, Niigata 951-8514, Japan; maedat@dent.niigata-u.ac.jp (T.M.)
* Correspondence: tanuma@dent.niigata-u.ac.jp (J.-I.T.); Tel.: +81-25-227-2832

Simple Summary: The early detection and treatment of oral squamous cell carcinoma will lead to improved postoperative quality of life; however, candidate biomarkers for the early detection of malignant transformation have not been identified. This may be partly because there is no experimental method that allows the continuous observation of molecular changes in the dysplasia-carcinoma sequence in the same individual. Oral cytology is a noninvasive diagnostic modality for the early detection of oral squamous cell carcinoma. Using liquid-based cytology techniques with the 4-nitroquinoline 1-oxide-induced rat tongue cancer model, we detected morphological changes and the expression patterns of candidate genes at the mRNA and protein levels in the same individual during carcinogenesis. BRD4 and c-Myc were useful biomarkers for the early detection of oral squamous cell carcinoma.

Abstract: Most oral squamous cell carcinomas (OSCCs) arise from oral epithelial dysplasia; however, there is no useful marker for early OSCC detection, likely owing to the inability to continuously observe the carcinoma sequence. We aimed to establish an experimental model to observe changes in the sequential expression pattern of mRNA and protein in the same rat using liquid-based cytology techniques. Cytology specimens were collected from a 4-nitroquinoline 1-oxide-induced rat tongue cancer model at 2, 5, 8, 11, 14, 17, and 21 weeks. We examined candidate biomarker expression using immunocytochemistry and quantitative real-time PCR. The percentage of positively stained nuclei was calculated as the labeling index (LI). All rats had OSCC of the tongue at 21 weeks. Brd4 (Brd4), Myc (c-Myc), and Tp53 (p53) mRNA levels were upregulated during progression from negative for intraepithelial lesion or malignancy to SCC. Brd4- and c-Myc-LI were increased in low- and high-grade squamous intraepithelial lesions and SCC specimens. p53-LI was significantly increased in SCC specimens. Our experimental model allowed the observation of sequential morphological changes and mRNA and protein expression patterns in the same rat during carcinogenesis. By reducing the false negative rate, BRD4 and c-Myc can be useful markers for the early detection of OSCC.

Keywords: oral squamous cell carcinoma; oral cancer; Brd4; c-Myc; p53; cytology; liquid-based cytology; immunocytochemistry; 4-nitroquinoline 1-oxide.

1. Introduction

Rates of oral squamous cell carcinoma (OSCC) incidence have increased to more than 355 000 new patients and 177 000 deaths annually worldwide [1-3]. The most common

sites for intraoral cancer are the tongue, gingiva, and floor of the mouth, accounting for more than half of all OSCCs [1]. The oral cavity is central to several essential functions such as speech, breathing, and feeding, and cancers in this region might be expected to have several effects on day-to-day life [4]. Early detection and treatment of OSCC will lead to improved postoperative quality of life. It is well-known that most OSCCs arise from oral epithelial dysplasia (OED), and while there have been studies on the detection of OSCC, candidate biomarkers for the early detection of malignant transformation have not been identified [5]. This may be partly because there is no experimental method that allows continuous observation of molecular changes in the dysplasia-carcinoma sequence in the same individual [6].

Liquid-based cytology (LBC) is a non-invasive technique that can be used to diagnose OED and OSCC. However, the false negative rate (FNR) has been reported to be 15.1–31.3% [7-10]; in particular, Kondo et al. [10] showed that 81% cases of mild or moderate dysplasia were cytologically diagnosed as negative for any intraepithelial lesion or malignancy (NILM). False negative results can lead to undiagnosed carcinoma progression and mortality, if no further treatments are undertaken. Therefore, decreasing the FNR (especially that of NILM) will improve the diagnostic accuracy of cytology. Although various methods, such as the additional oral Bethesda system of atypical squamous cells or argyrophilic nucleolar organizer region counting, have been employed to reduce the FNR of oral cytology, no effective method to reduce the FNR has been obtained [10,11].

Animal experiments are a useful method to observe molecular expression changes in the carcinogenesis process. We previously reported that Dark-Agouti (DA) rats are highly susceptible to 4-nitroquinoline 1-oxide (4NQO)-induced tongue cancer (TC) [12-14]. Moreover, DA rats with 4NQO induced TC are considered an ideal experimental model for human TC, because both tumors share several morphological and molecular biological properties [14]. Using LBC techniques on this model, it is theoretically possible to continuously observe malignant transformation events in the same rat. From other studies on 4NQO-induced TC, we selected Myc (c-Myc) and Tp53 (p53) as candidate genes for the early detection of OSCC [15,16]. In addition to these, we added bromodomain protein 4 (Brd4) as a candidate gene because Myc is transcriptionally regulated by Brd4 [17].

BRD4 is a member of the bromodomain and extraterminal domain (BET) family of transcriptional regulatory proteins and plays a key role in carcinogenesis and cancer progression [18]. Other studies detected significantly higher levels of Brd4 mRNA and protein in head and neck squamous cell carcinoma (SCC) tissues than in normal tissues [19-21]. Brd4 activates the transcription of oncogenes, including Myc, and is involved in cell proliferation [18]. c-Myc plays a key role in cell proliferation, metabolism, differentiation, and apoptosis, and its expression levels are associated with advanced stage OSCC and advanced degree of OED [18,22,23]. Moreover, high expression of c-Myc and p53 was observed in the early stages of oral carcinogenesis, and these markers proved useful tools for the early detection of premalignant lesions using immunohistochemistry (IHC) [24]. However, no studies have explored the application of these markers to immunocytochemistry (ICC).

The purpose of the present study was to establish an experimental model in which the sequential expression patterns of mRNA and protein could be observed in the same rat using LBC in a 4NQO-induced rat TC model, and to identify biomarkers that can reduce the FNR in ICC by continuously observing changes in the mRNA and protein levels of Brd4, c-Myc, and p53.

2. Materials and Methods

2.1. Animals

Inbred DA rats (DA/Slc) were purchased from the Shizuoka Laboratory Animal Center (Hamamatsu, Japan). Throughout the experiment, all rats were housed in a controlled environment with a 12 h light/dark cycle and temperature of 22 ± 2 ℃, and fed a

 doi:10.20944/preprints202107.0553.v1

commercial pellet (Nosan, Yokohama, Japan). Fifty-one male DA rats, 4 weeks old, were observed. This present study was reviewed by the Committee of the Ethics on Animal Experiment in Niigata University and carried out according to the Guidelines for Animal Experiment in Niigata University, Niigata, Japan (SA00507). All experiments also have been conducted in accordance with relevant national legislation on the use of animals for research.

2.2. TC induction

A stock solution of 4NQO (Nacalai Tesque Inc., Kyoto, Japan) at a concentration of 200 mg/L in 5% ethanol was prepared and stored at 4°C until use. Starting at 6 weeks of age, all rats were given drinking water containing 0.001% 4NQO ad libitum. Cytology specimens were taken from all rats at 2, 5, 8, 11, 14, 17 and 21 weeks. All rats were sacrificed at week 21 of the experiment. Full necropsy and histopathological examinations were performed. Three rats were used as controls and were not administered 4NQO. At 21 weeks, spontaneous tumors were not observed in the control rats.

2.3. LBC specimens

LBC samples were collected from the tongue region of rats. An Orcellex brush (Rovers Medical Devices B.V., Oss, Netherlands) or interdental brush was rotated on the lesional surface 20 times, and the collected contents were transferred into a methanol-based preservative solution (SurePath, BD Diagnostics, Franklin Lakes, NJ, USA) or RNAlater reagent (Ambion, Austin, TX, USA). LBC preparations were processed according to the manufacturer's protocol [25]. Fixed specimens were rehydrated with distilled water. Following this, nuclear staining with hematoxylin solution and cytoplasmic staining with Orange G solution (Muto Pure Chemicals Co., Ltd, Tokyo, Japan) and Eosin Azure solution (Muto Pure Chemicals Co., Ltd.) were performed. Cytological diagnosis was based on the oral Bethesda system [26].

2.4. Immunostaining methods for Brd4, c-Myc, and p53 in histology and cytology

Histologic sections were prepared at 4-μm thickness from each paraffin archival block and mounted on treated slides. Before labeling, slides were subjected to antigen retrieval in a microwave oven, with a maximum strength of 1000 W, using EDTA (pH 8.0) for 20 min followed by incubation with rabbit polyclonal anti-p53 antibody (1:50 dilution at room temperature (RT, 24 ± 2 ℃) for 2 h; clone ab131442; Abcam, Cambridge, MA, USA), rabbit monoclonal anti-c-Myc antibody (1:100 dilution at RT for 2 h; clone ab32072; Abcam), or rabbit monoclonal anti-BRD4 antibody (1:100 dilution at RT for 2 h; clone ab128874; Abcam). The slides were then washed and incubated with the Envision+/HRP system (Dako, Glostrup, Denmark). Immunoreactive cells were visualized using DAB (Dojindo, Kumamoto, Japan) followed by a hematoxylin counterstain.

2.5. Labeling index analysis of ICC

The percentages of positively stained nuclei for each of the antibodies (Brd4, c-Myc, and p53) were calculated as the labeling index (LI) in each captured image at ×200 magnification using e-Count2 cell counting software (e-Path, Kanagawa, Japan). Six random fields containing an average of 200 cells each were selected for analysis, and the average value for LI was calculated.

2.6. RNA isolation and qRT-PCR

The LBC specimens in the RNAlater reagent were isolated using the NucleoSpin RNA XS-kit (Macherey-Nagel, Düren, Germany) according to the manufacturer's instructions. The isolated RNA was eluted in 10 μL of RNase-free water and then the genomic DNA was eliminated using recombinant rDNase provided in the kit. Reverse transcription was then carried out using the High-Capacity cDNA Reverse Transcription Kit with RNase inhibitor (Applied Biosystems, Foster City, CA, USA) according to the manufacturer's standard protocol in a final volume of 20 μL. The program used was as follows: 25 °C for 10 min, 37 °C for 120 min, and 85 °C for 5 min. cDNA was amplified by PCR using

 doi:10.20944/preprints202107.0553.v1

a TaqMan Universal PCR Master Mix (Applied Biosystems) and TaqMan Gene Expression Assays (Applied Biosystems) with Brd4 (Rn01535560_m1), Myc (Rn07310910_m1) and Tp53 (Rn00755717_m1); 18S mRNA (Hs99999901_s1) was employed as the internal standard [27].

2.7. Semiquantitative analysis of target gene expression

To compare the levels of target gene transcripts in low-grade squamous intraepithelial lesion (LSIL), high-grade squamous intraepithelial lesion (HSIL) and SCC samples with those in NILM samples, their Ct (threshold cycle) values were first normalized by subtracting the Ct value of the 18S control (ΔCt=Ct,target - Ct,control). Overexpression of the selected gene transcripts in target samples was calculated by subtracting the normalized median ΔCt of the target samples with that of the NILM samples (ΔΔCt = median ΔCt,LSIL/HSIL/SCC - median ΔCt,NILM). Overexpression ratios were calculated as $2^{-\Delta\Delta Ct}$.

2.8. Statistical analysis

As the Shapiro-Wilk tests showed that the Brd4, c-Myc, and p53 LI and the Brd4 and Tp53 mRNA levels were always normally distributed, we tested these data parametrically. We used ANOVA with a post-hoc Tukey test for comparisons between multiple groups. In contrast, the Shapiro-Wilk tests showed that the Myc mRNA levels were not always normally distributed; therefore, we tested this data non-parametrically. The correlation between mRNA expression and LI was assessed using the Spearman rank correlation test. We evaluated the diagnostic ability of these biomarkers using receiver operating characteristic (ROC) curves. As a global measure for the accuracy of diagnosis, we also calculated the area under the ROC curve (AUC) for each individual biomarker. The optimal cut-off values for LI of Brd4, c-Myc, and p53 were determined using closest-topleft [28]. All statistical comparisons were performed using GraphPad Prism for Windows version 6.00 (GraphPad Software Inc., San Diego, CA, USA) and R version 4.0.2 (R Foundation, Vienna, Austria). A p value < 0.05 was considered significant, and all statistical tests were two-sided.

3. Results

3.1. Sample collection

In total, 357 cytology specimens were collected from the tongues of 51 rats. Those specimens were cytologically evaluated and classified into four groups according to the oral Bethesda system: NILM (n = 229), LSIL (n = 56), HSIL (n = 19), and SCC (n = 53). LSIL was recognized after the 11th week of treatment with 4NQO. At the 17th week, all the diagnostic classifications, from NILM to SCC, could be recognized. Finally, all the samples from the rats were evaluated as SCC at 21 weeks. The results of the cytopathological examination are summarized in Table 1. Histopathologically, all rats were diagnosed with SCC, which developed on the dorsum of the tongue; therefore, the cytological diagnosis was consistent with the histopathological diagnosis (Fig. 1).

Table 1. Cytological diagnoses of 51 rats each week.

Cytological diagnosis	4NQO treatment period (weeks)						
	2	5	8	11	14	17	21
NILM (n = 229)	51 (100%)	51 (100%)	51 (100%)	44 (86.3%)	25 (49.0%)	7 (13.7%)	0 (0.0%)
LSIL (n = 56)	0 (0.0%)	0 (0.0%)	0 (0.0%)	7 (13.7%)	25 (49.0%)	24 (47.1%)	0 (0.0%)
HSIL (n = 19)	0 (0.0%)	0 (0.0%)	0 (0.0%)	0 (0.0%)	1 (2.0%)	18 (35.3%)	0 (0.0%)
SCC (n = 53)	0 (0.0%)	0 (0.0%)	0 (0.0%)	0 (0.0%)	0 (0.0%)	2 (3.9%)	51 (100%)

Abbreviations: 4NQO, 4-nitroquinoline 1-oxide; NILM, negative for intraepithelial lesion or malignancy; LSIL, low-grade squamous intraepithelial lesion; HSIL, high-grade squamous intraepithelial lesion; SCC, squamous cell carcinoma.

 doi:10.20944/preprints202107.0553.v1

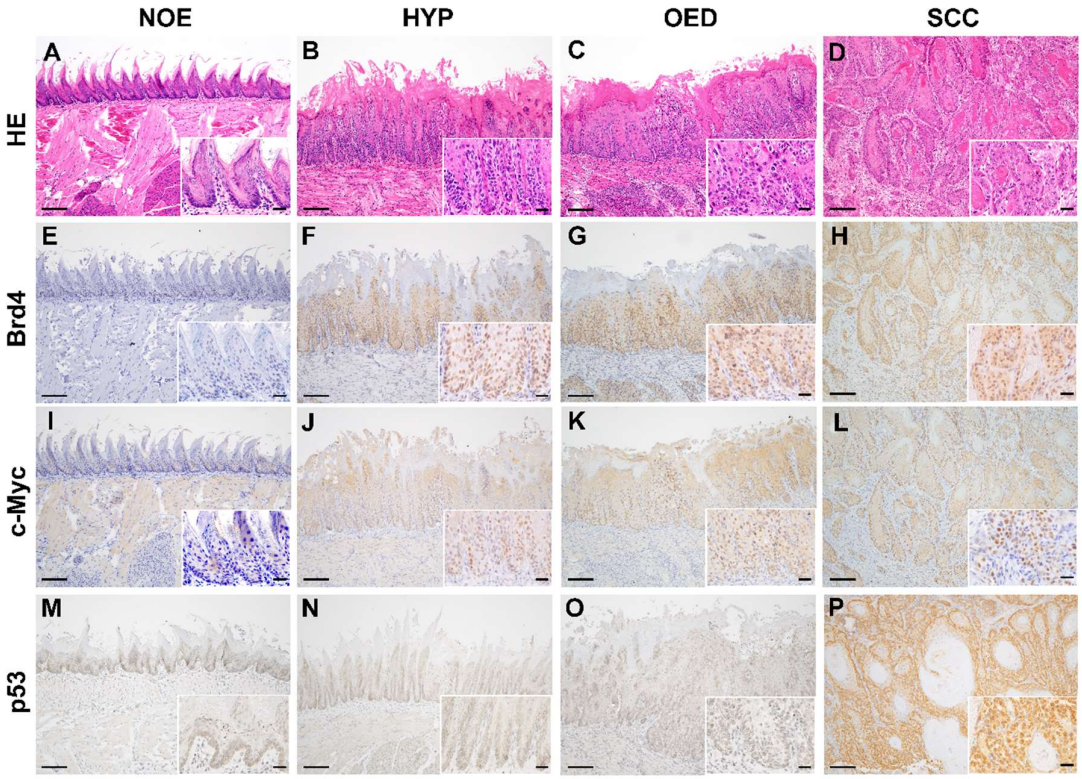

Figure 1. Representative histopathological and immunohistochemical findings of BRD4, c-Myc and p53 expression patterns in controls and 4NQO-treated rats at 21 weeks: normal epithelium (NOE) (**A**, **E**, **I**, **M**), hyperplasia (HYP) (**B**, **F**, **J**, **N**), oral epithelium dysplasia (OED) (**C**, **G**, **K**, **O**), and squamous cell carcinoma (SCC) (**D**, **H**, **L**, **P**); hematoxylin and eosin (HE) (**A**-**D**), Brd4 (**E**-**H**), c-Myc (**I**-**L**), and p53 (**M**-**P**). Original magnification, ×100 and ×400 (inset). Scale bars, 100 μm and 20 μm (inset).

3.2. Immunoexpression of Brd4, c-Myc, and p53 in IHC and ICC

By IHC staining, we evaluated the expression of Brd4, c-Myc, and p53. Brd4 was expressed from the basal layer to the superficial layer in the hyperplasia, OED, and OSCC tissue specimens (Fig. 1E-H). Expression of c-Myc was limited to the basal and parabasal layers of the hyperplasia. c-Myc-positive cells were observed from the basal layer to the superficial layers in the OED and OSCC tissue specimens (Fig. 1I-L). Diffuse and intensive nuclear positivity of p53 was detected in OSCC tissue specimens but was absent in the normal mucosal epithelium, hyperplasia, and OED tissue specimens(Fig. 1M-P).

In Papanicolaou staining, NILM specimens exhibited orangeophilic keratinized cells without atypical or higher brightness (Fig. 2A). LSIL specimens had mild atypical high-bright orangeophilic keratinized cells (Fig. 2B), whereas the HSIL specimens had moderate atypical high-bright orangeophilic keratinized cells (Fig. 2C). Many atypical parabasal/basal cell clusters were detected in SCC specimens (Fig. 2D). NILM, LSIL, HSIL, and SCC in LBC specimens were evaluated by performing ICC staining for Brd4, c-Myc, and p53. NILM specimens were mostly negative for these markers (Fig. 3A, 4A, 5A). In LSIL and HSIL specimens, positive staining of Brd4 and c-Myc was observed in the atypical enlarged nuclei of the superficial and intermediate cells (Fig. 3B, 3C, 4B, 4C). In SCC specimens, Brd4 and c-Myc were detected in parabasal/basal cells appearing small and rounded with nuclear changes, such as nuclear enlargement, nuclear shape abnormalities, and increased nuclear to cytoplasmic ratios (Fig. 3C, 3D). In contrast, p53 was found only in SCC specimens, and p53-positive cells were localized in the atypical nucleus of parabasal/basal cells (Fig. 5B-D).

 doi:10.20944/preprints202107.0553.v1

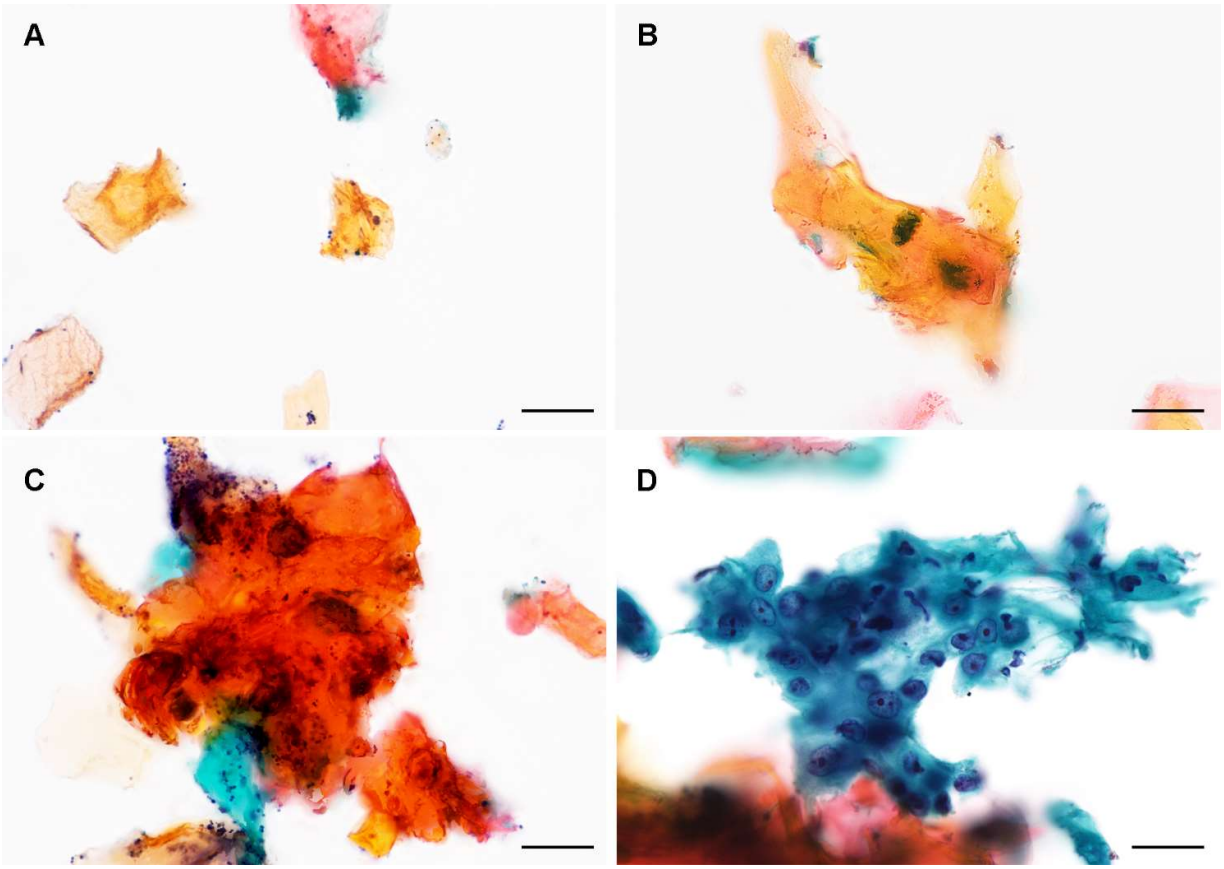

Figure 2. Representative cytological findings of Papanicolaou stains in liquid-based cytology specimens: negative for intraepithelial lesion or malignancy (NILM) (**A**), low-grade squamous intraepithelial lesion (LSIL) (**B**), high-grade squamous intraepithelial lesion (HSIL) (**C**), and squamous cell carcinoma (SCC) (**D**). Original magnification, ×600. Scale bars, 20 μm.

 doi:10.20944/preprints202107.0553.v1

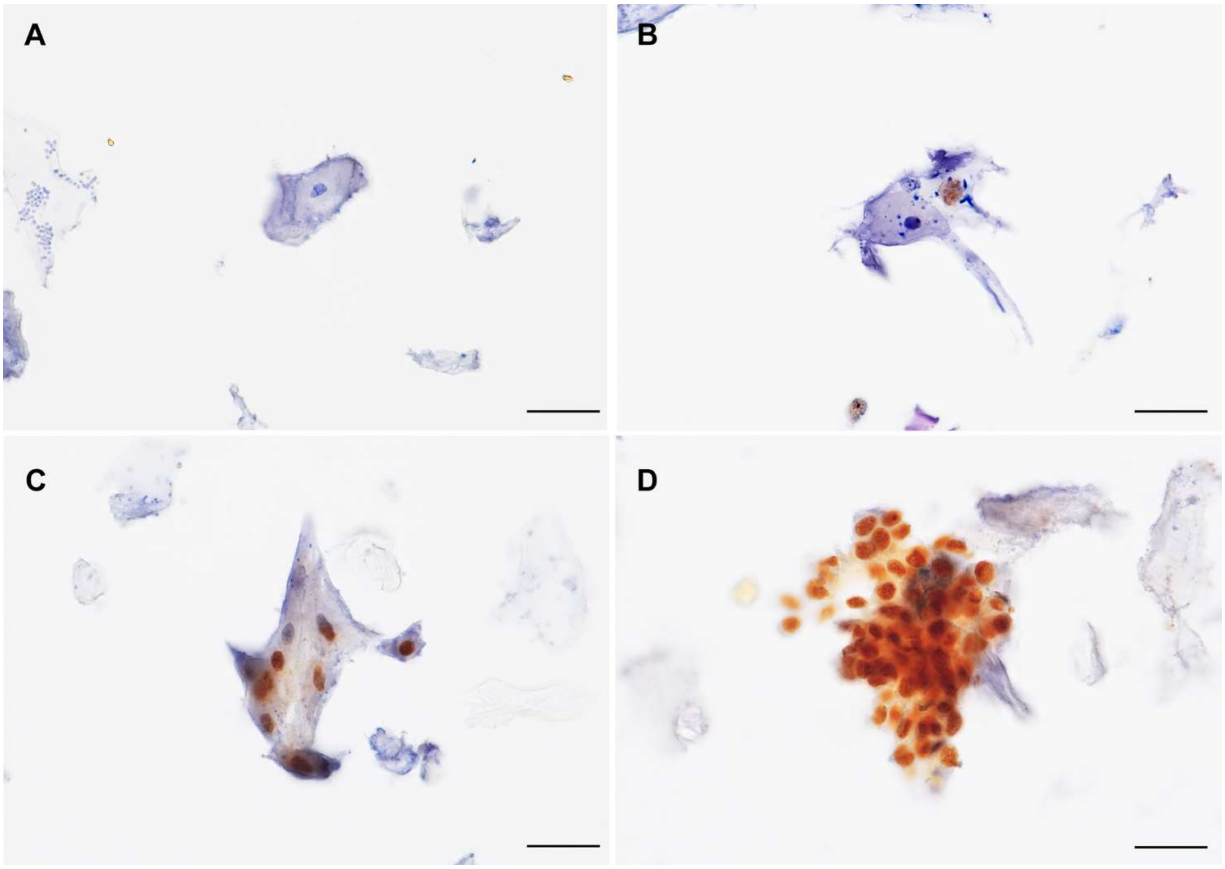

Figure 3. Brd4 immunocytochemical staining for oral smears (**A**-**D**). Although Brd4 staining generally was negative in NILM (**A**) specimens, positive staining in the nuclei was observed in LSIL (**B**), HSIL (**C**), and SCC (**D**) specimens. Original magnification, ×600. Scale bars, 20 μm.

 doi:10.20944/preprints202107.0553.v1

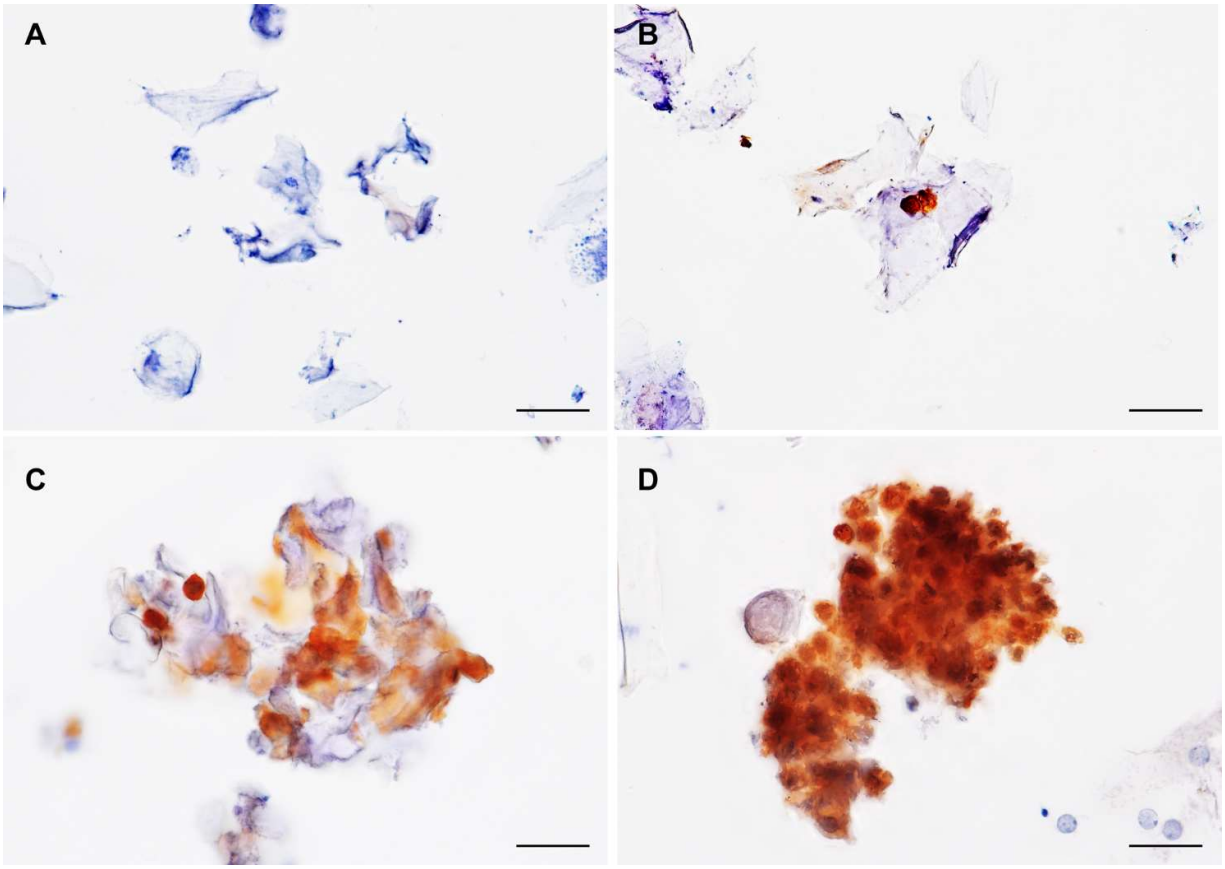

Figure 4. c-Myc immunocytochemical staining for oral smears (**A**-**D**). Although c-Myc staining was generally negative in NILM (**A**) specimens, positive staining in the nuclei was observed in LSIL (**B**), HSIL (**C**), and SCC (**D**) specimens. Original magnification, ×600. Scale bars, 20 μm.

 doi:10.20944/preprints202107.0553.v1

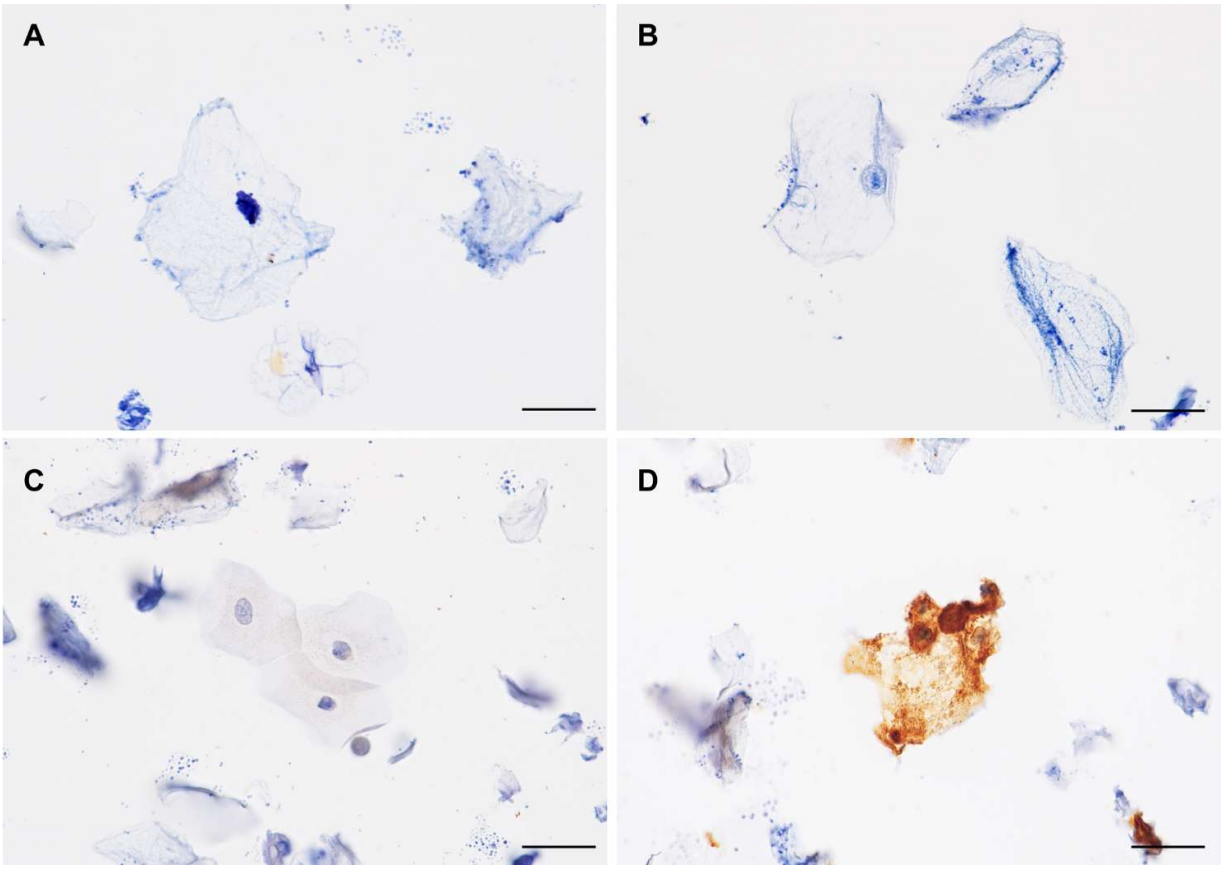

Figure 5. p53 immunocytochemical staining for oral smears (**A**-**D**). Although p53 staining was generally negative in NILM (**A**), LSIL (**B**), and HSIL (**C**) specimens, positive staining in the nuclei was observed in SCC (**D**) specimens. Original magnification, ×600. Scale bars, 20 μm.

3.3. Analysis of mRNA expression level of candidate markers in LBC specimens

qRT-PCR for Brd4, c-Myc, and p53 revealed a statistically significant difference in the mRNA expression level of each marker among the oral Bethesda categories ($p < 0.01$; Tukey's multiple comparisons test (Brd4 and Tp53), Kruskal-Wallis test (Myc)). In addition, the levels of Brd4, Myc, and Tp53 mRNAs were significantly higher in SCC specimens than in NILM, LSIL, and HSIL specimens ($p < 0.01$; Fig. 6A-C). These results showed that these mRNAs were upregulated during the carcinogenesis process of 4NQO-induced TC.

 doi:10.20944/preprints202107.0553.v1

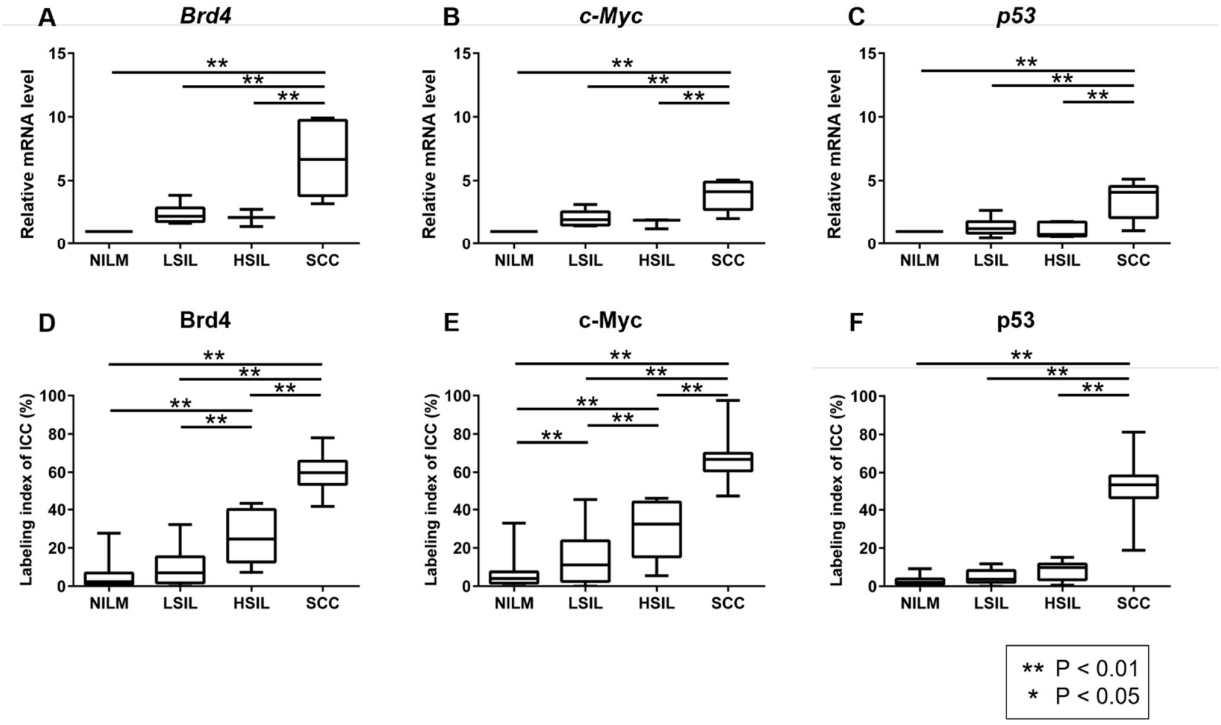

Figure 6. Box plots showing normalized expression of Brd4 (**A**), c-Myc (**B**), and p53 (**C**) in NILM, LSIL, HSIL, and SCC specimens. The box represents 50% quartiles (above 25% and below 75%) and the solid line within each box is the median gene expression value. Tukey's multiple comparisons test and the Kruskal-Wallis test were used to determine statistical significance. Boxplots for labeling indices from immunocytochemistry (ICC) of Brd4 (**D**), c-Myc (**E**), and p53 (**F**) in NILM, LSIL, HSIL, and SCC specimens. Tukey's multiple comparisons test was used to determine statistical significance.

3.4. Analysis of protein levels of candidate markers in LBC specimens

To identify Brd4, c-Myc, and p53 protein expression patterns in the grades of the oral Bethesda category, we next analyzed the expression of Brd4, c-Myc, and p53 proteins in NILM, LSIL, HSIL, and SCC specimens using ICC. Tukey's multiple comparisons test showed a significant difference in the LI of Brd4 (BRD4-LI), c-Myc (c-Myc-LI), and p53 (p53-LI) among the oral Bethesda categories ($p < 0.01$). The BRD4-LI was significantly higher in HSIL and SCC specimens than in NILM and LSIL specimens based on ICC results ($p < 0.01$; Tukey's multiple comparisons test) (Fig. 6D). In line with Brd4, c-Myc-LI was significantly higher in HSIL and SCC specimens than in NILM and LSIL specimens ($p < 0.01$; Tukey's multiple comparisons test) (Fig. 6E). As for p53, p53-LI was significantly higher in SCC specimens than in NILM, LSIL, and HSIL specimens ($p < 0.01$; Tukey's multiple comparisons test). These results showed that the expression of these proteins increased with disease severity. In particular, the levels of Brd4 and c-Myc were found to be higher in LSIL and HSIL specimens.

3.5. Relationship between expression level of mRNA and LI of Brd4, c-Myc and p53

To analyze the relationship between expression levels of mRNA and LI, we assessed correlations for each candidate marker. Figure 7 shows the relationship between Brd4, c-Myc, and p53 mRNA expression levels and LI. Significant correlations were detected for Brd4 ($r = 0.761$, $p < 0.01$, Fig. 7A), c-Myc ($r = 0.794$, $p < 0.01$, Fig. 7B) and p53 ($r = 0.599$, $p < 0.01$, Fig. 7C).

Preprints (www.preprints.org) | NOT PEER-REVIEWED | Posted: 26 July 2021 doi:10.20944/preprints202107.0553.v1

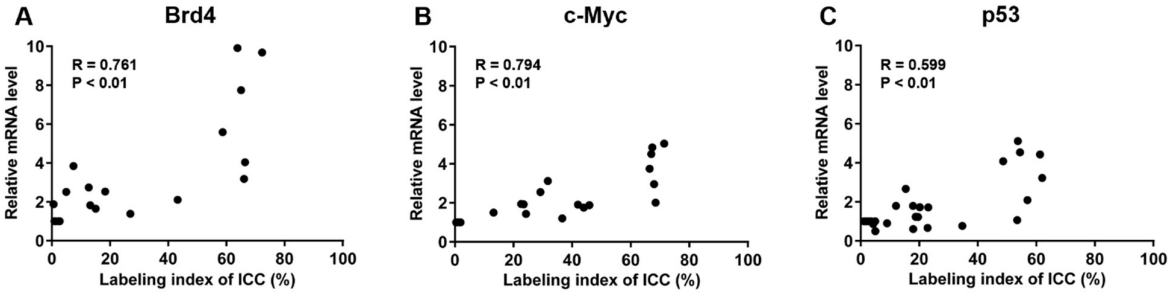

Figure 7. Correlation between labeling index and relative mRNA level of each marker (Brd4, c-Myc, p53) for cytology specimens. These markers displayed significant positive correlations (Brd4: r = 0.761, p = 0.000 (**A**); c-Myc: r = 0.794, p = 0.000 (**B**); p53: r = 0.599, p = 0.002 (**C**)).

3.6. Diagnostic accuracy of candidate markers

To evaluate the diagnostic accuracy of increased LI for individual candidate markers, we stratified the LI of each marker as positive (LI below cut-off) or negative (LI above the cut-off), and calculated the sensitivities and specificities to detect LSIL or a higher category by ROC analysis (Fig. 8). AUCs were 0.833 (standard error [SE]: 0.039; 95% CI: 0.758–0.909) for Brd4, 0.849 (SE: 0.036; 95% CI: 0.778–0.921) for c-Myc and 0.829 (SE: 0.042; 95% CI: 0.747–0.911) for p53. Table 2 shows the sensitivity, specificity, FNR, negative predictive value (NPV), positive predictive value (PPV), and diagnostic accuracy of all markers. By oral Bethesda category, cut-off BRD4-LI values greater than 5.99% were found in 60.0% of LSIL and 100% of HSIL specimens; likewise for c-Myc, cut-off c-Myc-LI values greater than 12.0% were found in 50.0% of LSIL and 78.0% of HSIL specimens. In contrast, a cut-off p53-LI greater than 3.6% was found in only 20% of LSIL and 58% of HSIL specimens.

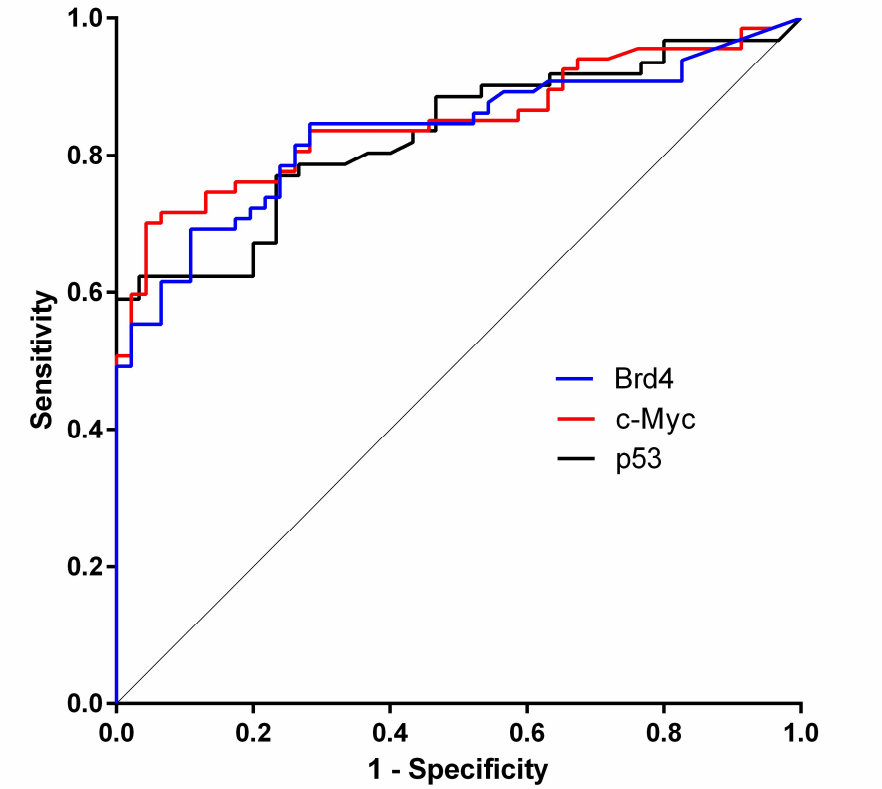

Figure 8. Receiver operating characteristic (ROC) analysis for LSIL or higher category specimens screening using Brd4 (blue line), c-Myc (red line), and p53 (black line) as candidate markers. The optimal cut-off values of each marker were calculated using closest-topleft [27].

 doi:10.20944/preprints202107.0553.v1

Table 2. Cut-Off values, sensitivity, specificity, false negative rates, negative predictive values, and positive predictive values of BRD4-LI, c-Myc-LI, and p53-LI

Markers	Cut-off value (%)	Sensitivity (%)	Specificity (%)	FNR (%)	PPV (%)	NPV (%)	Accuracy (%)
Brd4	5.99	81.5	73.9	18.5	81.5	73.9	78.3
c-Myc	12.0	74.6	87.0	25.3	89.3	70.2	79.6
p53	3.60	59.0	100	41.0	100	54.4	72.5

Abbreviations: Brd4, bromodomain protein 4; FNR, false negative ratio; PPV, positive predictive value; NPV, negative predictive value.

4. Discussion

To detect useful biomarkers for the early diagnosis of OSCC, we established a novel experimental rat model that could capture biological changes in a multi-step carcinogenesis process in the same rat. Papanicolaou smears showed that there was sequential progression from NILM to LSIL/HSIL to SCC, and these morphological changes resemble those found during the progression of human oral carcinogenesis. We also succeeded for the first time in performing ICC and mRNA isolation from cytology specimens of a 4NQO-induced rat TC model. Several studies have suggested that a 4NQO-induced rat TC model can be used to visualize histological as well as molecular changes in human oral carcinogenesis [14,29,30]; however, no study has observed morphological as well as molecular changes using cytology specimens. We believe this to be the first study demonstrating the changes in morphology and mRNA and protein expression in cytology specimens of a single individual during the carcinogenesis process.

qRT-PCR analysis showed that Brd4, Myc, and Tp53 mRNA expression increased with the progression from NILM to SCC, and each marker was significantly more highly expressed in SCC specimens than in NILM, LSIL, and HSIL specimens. These observations are in line with previous studies of OSCC [21,31,32]. For example, Wu et al. [21] reported that the level of Brd4 mRNA was aberrantly upregulated in head and neck SCC samples and a 4NQO-induced OSCC animal model. Several studies found that c-Myc and p53 were overexpressed in OSCC tissues and TSCCA and CAL-27 cell lines, compared with their levels in normal tissues and normal human oral keratinocytes cells [31,32].

In addition, the LI values of Brd4, c-Myc, and p53 were sequentially increased with the progression from NILM to SCC. Although c-Myc immunostaining patterns can be divided into three types—nuclear, granular perinuclear, and diffuse cytoplasmic—we only analyzed the nuclear-positive patterns. In frozen specimens of normal tissues, Loke et al. [33] found a predominant nuclear localization of c-Myc protein in the liver, spleen, brain, colonocytes, and lung; however, when tissues were fixed in formalin, this pattern was altered, suggesting possible protein translocation to the cytoplasm during fixation. Another study found that c-Myc is ubiquitinated in the nucleus and then exported to the cytoplasm for degradation [34]. As c-Myc is a nuclear transcription factor, it is most active when in the nucleus [35]. Although, there is still room for disagreement about the evaluation of the c-Myc expression pattern in OSCC, collectively, these studies indicate that the cytoplasmic localization of c-Myc immunoreactivity is unlikely to be considered positive, and it seems reasonable to evaluate the nuclear localization of c-Myc in OSCC. Moreover, the methods used for calculating LI were adequate because there was a significant correlation between the LI and mRNA expression level of each marker (Fig. 7).

The immunohistochemical staining results revealed the absence of p53 expression in the normal mucosal epithelium, hyperplasia, or OED specimens; thus, it was impossible to collect samples using cytology specimens. In contrast, hyperplasia, OED, and OSCC specimens showed expression of Brd4 from the basal to superficial layers. c-Myc was

expressed in the basal to mid-portion of the spinous layer in the hyperplasia specimens, and in the basal to superficial layer in the OED and SCC specimens; therefore, Brd4 and c-Myc could be detected by ICC at that time in the hyperplasia and OED specimens (Fig. 6D, 6E, 6F). ICC had a high capacity for the detection of positive cells compared with qRT-PCR, because ICC calculates the LI for the hot spots of the cytology specimens whereas qRT-PCR evaluates entire specimens. Consequently, ICC was shown to be a more useful method than qRT-PCR for the early detection of OSCC from cytology specimens.

BRD4-LI and c-Myc-LI were significantly increased in the early stages of the carcinogenesis process, and therefore, they may be good predictors of OSCC. Cytologic diagnoses based on morphologic changes are frequently difficult to determine due to false negatives. In particular, the distinction between reactive/regenerative or neoplastic changes, namely NILM and LSIL is challenging [36]. Our analysis showed that cells positive for Brd4 and c-Myc were more frequently detected in LSIL specimens than p53 was. Therefore, we consider that assessing BRD4-LI and c-Myc-LI by ICC, in addition to cytological diagnosis, has the potential to reduce the FNR of neoplastic change from oral cytology. Myc is well known as an oncogene and is a downstream target of Brd4 [18]. Although c-Myc promotes p53, it also induces cyclins D/E and cyclin-dependent protein kinases 2/4/6 and represses $p21^{CIP1}$ and $p27^{KIP1}$, leading to cell cycle progression [37-42]. Brd4 and c-Myc are usually upregulated in OSCC and are significantly associated with aggressive clinicopathological features and poor survival [18,43]. However, there is little research on whether they are useful markers for the early detection of OSCC. Combining cytology and ICC to increase diagnostic accuracy has also been widely researched in other locations, but few studies have been conducted in the oral cavity [34,44-49]. Our study thus offers a new cytological diagnosis tool for OSCC. In future studies, the efficacy of these markers will need to be tested in human cytology specimens and evaluated to improve diagnostic accuracy.

5. Conclusions

This novel experimental model allowed us to observe the sequential morphologic changes and expression patterns of mRNAs and proteins in the same rat during the carcinogenesis process. Our data also suggested that ICC-based detection of Brd4 or c-Myc from cytology specimens could be an improved diagnostic accuracy tool that, in combination with cytological diagnosis, has promising potential to improve the diagnostic accuracy of OSCC.

Author Contributions: Conceptualization, M.K., M.Y., S.M., T.A., and J.-I.T.; formal analysis, M.K., S.M., T.K., T.M., and J.-I.T.; investigation, M.K., M.Y., and J.-I.T.; methodology, M.K., S.M., and J.-I.T.; resources, M.K., M.Y., S.M., T.K., and J.-I.T.; data curation, M.K., N.N.C., and J.-I.T.; writing—original draft preparation, M.K. and J.-I.T.; writing—review and editing, All authors; visualization, M.K., M.Y., S.M., T.A., and J.-I.T.; supervision, M.K., T.K., T.M., and J.-I.T.; project administration, M.K., M.Y., S.M., T.A., and J.-I.T.; funding acquisition, J.-I.T.; All authors have read and agreed to the published version of the manuscript.

Funding: This research was funded by Grants-in-Aid for Scientific Research from the Japan Society for the Promotion of Science (JSPS KAKENHI Grant No. 19 K10069 to JT).

Institutional Review Board Statement: The study was approved by the Animal Experimentation Ethics Committee of Niigata University (SA 00507, 2019).

Data Availability Statement: The data presented in this study are available on request from the corresponding author.

Conflicts of Interest: The authors declare no conflicts of interest.

References

1. El-Naggar, A.K.; Chan, J.K.C.; Grandis, J.R.; Takata, T.; Slootweg, P.J; Eds. *World Health Organization Classification of Head and Neck Tumours*, 4th ed.; Lyon, France, **2017**; pp. 109-111, ISBN 978-92-832-2438-9.

2. Bray, F.; Ferlay, J.; Soerjomataram, I.; Siegel, R.L.; Torre, L.A.; Jemal, A. Global cancer statistics 2018: GLOBOCAN estimates of incidence and mortality worldwide for 36 cancers in 185 countries. *CA Cancer J. Clin.* **2018,** 68, 394-424, doi:10.3322/caac.21492.
3. Miranda-Filho, A.; Bray, F. Global patterns and trends in cancers of the lip, tongue and mouth. *Oral Oncol.* **2020**, 102, 104551, doi:10.1016/j.oraloncology.2019.104551.
4. Tirelli, G.; Gatto, A.; Bonini, P.; Tofanelli, M.; Arnež, Z.M.; Piccinato, A. Prognostic indicators of improved survival and quality of life in surgically treated oral cancer. *Oral Surg. Oral Med. Oral Pathol. Oral Radiol.* **2018**, 126, 31-40, doi:10.1016/j.oooo.2018.01.016.
5. Blatt, S.; Krüger, M.; Ziebart, T.; Sagheb, K.; Schiegnitz, E.; Goetze, E.; Al-Nawas, B.; Pabst, A.M. Biomarkers in diagnosis and therapy of oral squamous cell carcinoma: A review of the literature. *J. Craniomaxillofac. Surg.* **2017**, 45, 722-730, doi:10.1016/j.jcms.2017.01.033.
6. Omar, E. Current concepts and future of noninvasive procedures for diagnosing oral squamous cell carcinoma - a systematic review. *Head Face Med.* **2015**, 11, 6, doi:10.1186/s13005-015-0063-z.
7. Deuerling, L.; Gaida, K.; Neumann, H.; Remmerbach, TW. Evaluation of the accuracy of liquid-based oral brush cytology in screening for oral squamous cell carcinoma. *Cancers (Basel)* **2019**, 11, 1813, doi:10.3390/cancers11111813.
8. Alsarraf, A.; Kujan, O.; Farah, CS. Liquid-based oral brush cytology in the diagnosis of oral leukoplakia using a modified Bethesda Cytology system. *J. Oral Pathol. Med.* **2018**, 47, 887-894, doi:10.1111/jop.12759.
9. Remmerbach, T.W.; Pomjanski, N.; Bauer, U.; Neumann, H. Liquid-based versus conventional cytology of oral brush biopsies: a split-sample pilot study. *Clin. Oral Investig.* **2017**, 21, 2493-2498, doi:10.1007/s00784-017-2047-9.
10. Kondo, Y.; Oya, K.; Sakai, M.; Fujiwara, C.; Tojo, F.; Usami, Y.; Fukuda, Y.; Kogo, M.; Kishino, M. Accuracy of liquid-based cytology (LBC) in the oral mucosa according to novel diagnostic guidelines in Japan: Classification of cytology for oral mucosal disease. *Oral Sci. Int.* **2020**, 17, 22-28, doi:10.1002/osi2.1035.
11. Jajodia, E.; Raphael, V.; Shunyu, N.B.; Ralte, S.; Pala, S.; Jitani, A.K. Brush Cytology and AgNOR in the Diagnosis of Oral Squamous Cell Carcinoma. *Acta Cytol.* **2017**, 61, 62-70, doi:10.1159/000451050.
12. Tanuma, J.I.; Shisa, H.; Hiai, H.; Higashi, S.; Yamada, Y.; Kamoto, T.; Hirayama, Y.; Matsuuchi, H.; Kitano, M. Quantitative trait loci affecting 4-nitroquinoline 1-oxide-induced tongue carcinogenesis in the rat. *Cancer Res.* **1998**, 58, 1660-1664.
13. Tanuma, J.I.; Kitano, M.; Shisa, H.; Hiai, H. Polygenetic susceptibility and resistance to 4-nitroquinoline 1-oxide-induced tongue carcinomas in the rat. *J. Exp. Anim. Sci.* **2000**, 41, 68-77, doi:10.1016/S0939-8600(00)80034-6.
14. Tanuma, J.I.; Hiai, H.; Shisa, H.; Hirano, M.; Semba, I.; Nagaoka, S.; Kitano, M. Carcinogenesis modifier loci in rat tongue are subject to frequent loss of heterozygosity. *Int. J. Cancer* **2002**, 102, 638-642, doi:10.1002/ijc.10751.
15. Tang, X.H.; Urvalek, A.M.; Osei-Sarfo, K.; Zhang, T.; Scognamiglio, T.; Gudas, L.J. Gene expression profiling signatures for the diagnosis and prevention of oral cavity carcinogenesis-genome-wide analysis using RNA-seq technology. *Oncotarget* **2015**, 6, 24424-24435, doi:10.18632/oncotarget.4420.
16. Okazaki, Y.; Tanaka, Y.; Tonogi, M.; Yamane, G. Investigation of environmental factors for diagnosing malignant potential in oral epithelial dysplasia. *Oral Oncol.* **2002**, 38, 562-573, doi:10.1016/s1368-8375(01)00119-1.
17. Zuber, J.; Shi, J.; Wang, E.; Rappaport, AR.; Herrmann, H.; Sison, E.A.; Magoon, D.; Qi, J.; Blatt, K.; Wunderlich, M.; Taylor, M.J.; Johns, C.; Chicas, A.; Mulloy, J.C.; Kogan, S.C.; Brown, P.; Valent, P.; Bradner, J.E.; Lowe, S.W.; Vakoc, C.R. RNAi screen identifies Brd4 as a therapeutic target in acute myeloid leukaemia. *Nature* **2011**, 478, 524-528, doi:10.1038/nature10334.
18. Lovén, J.; Hoke, HA.; Lin, C.Y.; Lau, A.; Orlando, D.A.; Vakoc, C.R.; Bradner, J.E.; Lee, T.I.; Young, R.A. Selective inhibition of tumor oncogenes by disruption of super-enhancers. *Cell* **2013**, 153, 320-334, doi:10.1016/j.cell.2013.03.036.
19. Liu, X.; Li, Q.; Huang, P.; Tong, D.; Wu, H.; Zhang, F. EGFR-mediated signaling pathway influences the sensitivity of oral squamous cell carcinoma to JQ1. *J. Cell Biochem.* **2018**, 119, 8368-8377, doi:10.1002/jcb.26920.
20. Zhao, L.; Li, P.; Zhao, L.; Wang, M.; Tong, D.; Meng, Z.; Zhang, Q.; Li, Q.; Zhang, F. Expression and clinical value of PD-L1 which is regulated by BRD4 in tongue squamous cell carcinoma. *J. Cell Biochem.* **2020**, 121, 1855-1869, doi:10.1002/jcb.29420.
21. Wu, Y.; Wang, Y.; Diao, P.; Zhang, W.; Li, J.; Ge, H.; Song, Y.; Li, Z.; Wang, D.; Liu, L.; Jiang, H.; Cheng, J. Therapeutic targeting of BRD4 in head neck squamous cell carcinoma. *Theranostics* **2019**, 9, 1777-1793, doi:10.7150/thno.31581.
22. Bretones, G.; Delgado, MD.; León, J. Myc and cell cycle control. *Biochim. Biophys. Acta* **2015**, 1849, 506-516.
23. Pérez-Sayáns, M.; Suárez-Peñaranda, J.M.; Pilar, G.D.; Barros-Angueira, F.; Gándara-Rey, J.M.; García-García, A. What real influence does the proto-oncogene c-myc have in OSCC behavior? *Oral Oncol.* **2011**, 47, 688-692, doi:10.1016/j.oraloncology.2011.05.016.
24. Papakosta, V.; Vairaktaris, E.; Vylliotis, A.; Derka, S.; Nkenke, E.; Vassiliou, S.; Lazaris, A.; Mourouzis, C.; Rallis, G.; Spyridonidou, S.; Anagnostopoulou, S.; Perrea, D.; Donta, I.; Yapijakis, C.; Patsouris, E. The co-expression of c-myc and p53 increases and reaches a plateau early in oral oncogenesis. *Anticancer Res.* **2006**, 26, 2957-2962.
25. Norimatsu, Y.; Yamaguchi, T.; Taira, T.; Abe, H.; Sakamoto, H.; Takenaka, M.; Yanoh, K.; Yoshinobu, M.; Irino, S.; Hirai, Y.; Kobayashi, K. Inter-observer reproducibility of endometrial cytology by the Osaki Study Group method: utilising the Becton Dickinson SurePathTM liquid-based cytology. *Cytopathology* **2016**, 27, 472-478, doi:10.1111/cyt.12342.
26. Suzuki, T.; Isaka, E.; Hiraga, C.; Akiyama, Y.; Okamura, M.; Oomura, Y.; Hashimoto, K.; Sato, K.; Tanaka, Y.; Nomura, T. New oral cytodiagnostic criteria predict change to oral epithelial dysplasia (OED) and cancerization. [published online ahead of print January 23, 2021]. *Oral Sci Int.* **2021**, doi:10.1002/osi2.1100.

27. Ogawa, K.; Tanuma, J.I.; Hirano, M.; Hirano, M.; Hirayama, Y.; Semba, I.; Shisa, H.; Kitano, M. Selective loss of resistant alleles at p15INK4B and p16INK4A genes in chemically-induced rat tongue cancers. *Oral Oncol.* **2006**, 42, 710-717, doi:10.1016/j.oraloncology.2005.11.011.
28. Robin, X.; Turck, N.; Hainard, A.; Tiberti, N.; Lisacek, F.; Sanchez, J.C.; Műller, M. pROC: an open-source package for R and S+ to analyze and compare ROC curves. *BMC Bioinformatics* **2011**, 8, 12-77, doi:10.1186/1471-2105-12-77.
29. Kanojia, D.; Vaidya, M.M. 4-Nitroquinoline-1-oxide induced experimental oral carcinogenesis. *Oral Oncol.* **2006**, 42, 655-667.
30. Moon, S.M.; Ahn, M.Y.; Kwon, S.M.; Kim, S.A.; Ahn, S.G.; Yoon, J.H. Homeobox C5 expression is associated with the progression of 4-nitroquinoline 1-oxide-induced rat tongue carcinogenesis. *J. Oral Pathol. Med.* **2012**, 41, 470-476, doi:10.1111/j.1600-0714.2012.01133.x.
31. Li, S.; Zhang, S.; Chen, J. c-Myc induced upregulation of long non-coding RNA SNHG16 enhances progression and carcinogenesis in oral squamous cell carcinoma. *Cancer Gene Ther.* **2019**, 26, 400-410, doi:10.1038/s41417-018-0072-8.
32. Ota, K.; Fujimori, H.; Ueda, M.; Jono, H.; Shinriki, S.; Ota, T.; Sueyoshi, T.; Taura, M.; Taguma, A.; Kai, H.; Shinohara, M.; Ando, Y. Midkine expression is correlated with an adverse prognosis and is down-regulated by p53 in oral squamous cell carcinoma. *Int. J. Oncol.* **2010**, 37, 797-804, doi:10.3892/ijo_00000729.
33. Loke, S.L.; Neckers, L.M.; Schwab, G.; Jaffe, E.S. c-myc Protein in normal tissue. Effects of fixation on its apparent subcellular distribution. *Am. J. Pathol.* **1988**, 131, 29-37.
34. Lee, C.M. Transport of c-MYC by Kinesin-1 for proteasomal degradation in the cytoplasm. Biochim. Biophys. Acta **2014**, 1843, 2027-2036, doi:10.1016/j.bbamcr.2014.05.001.
35. Pérez-Sayáns, M.; Suárez-Peñaranda, J.M.; Padín-Iruegas, E.; Gayoso-Diz, P.; Almeida, M.R.D.; Barros-Anguira, F.; Gándara-Vila, P.; Blanco-Carrión, A.; García-García, A. Quantitative determination of c-myc facilitates the assessment of prognosis of OSCC patients. *Oncol. Rep.* **2014**, 31, 1677-1682, doi:10.3892/or.2014.3040.
36. Noda, Y.; Kondo, Y.; Sakai, M.; Sato, S.; Kishino, M. Galectin-1 is a useful marker for detecting neoplastic squamous cells in oral cytology smears. *Hum. Pathol.* **2016**, 52, 101-109, doi:10.1016/j.humpath.2016.01.014.
37. Bouchard, C.; Dittrich, O.; Kiermaier, A.; Dohmann, K.; Menkel, A.; Eilers, M.; Lűscher, B. Regulation of cyclin D2 gene expression by the Myc/Max/Mad network: Myc-dependent TRRAP recruitment and histone acetylation at the cyclin D2 promoter. *Genes Dev.* **2001**, 15, 2042-2047, doi:10.1101/gad.907901.
38. Tumbarello, D.A.; Turner, C.E. Hic-5 Contributes to Transformation Through a RhoA / ROCK-dependent Pathway. *J. Cell. Physiol.* **2007**, 211, 736-747, doi:10.1002/jcp.20991.
39. Hermeking, H.; Rago, C.; Schuhmacher, M.; Li, Q.; Barrett, J.F.; Obaya, A.J.; O'Connell, B.C.; Mateyak, M.K.; Tam, W.; Kohlhuber, F.; Dang, C.V.; Sedivy, J.M.; Eick, D.; Vogelstein, B.; Kinzler, K.W. Identification of CDK4 as a target of c-MYC. *Proc. Natl. Acad. Sci. U.S.A.* **2000**, 97, 2229-2234, doi:10.1073/pnas.050586197.
40. Yap, C.S.; Peterson, A.L.; Castellani, G.; Sedivy, J.M.; Neretti, N. Kinetic profiling of the c-Myc transcriptome and bioinformatic analysis of repressed gene promoters. *Cell Cycle* **2011**, 10, 2184-2196, doi:10.4161/cc.10.13.16249.
41. Claassen, G.F.; Hann, S.R. A role for transcriptional repression of p21CIP1 by c-Myc in overcoming transforming growth factor β-induced cell-cycle arrest. *Proc. Natl. Acad. Sci. U.S.A.* **2000**, 97, 9498-9503, doi:10.1073/pnas.150006697.
42. Acosta, J.C.; Ferrándiz, N.; Bretones, G.; Torrano, V.; Blanco, R.; Richard, C.; O'Connell, B.; Sedivy, J.; Delgado, M.D.; León, J. Myc Inhibits p27-Induced Erythroid Differentiation of Leukemia Cells by Repressing Erythroid Master Genes without Reversing p27-Mediated Cell Cycle Arrest. *Mol. Cell. Biol.* **2008**, 28, 7286-7295, doi:10.1128/MCB.00752-08.
43. Waitzberg, A.F.L.; Nonogaki, S.; Nishimoto, I.N.; Kowalski, L.P.; Miguel, R.E.V.; Brentani, R.R.; Brentani, M.M. Clinical significance of c-myc and p53 expression in head and neck squamous cell carcinomas. *Cancer Detect. Prev.* **2004**, 28, 178-186, doi:10.1016/j.cdp.2004.02.003.
44. Vlajnic, T.; Savic, S.; Barascud, A.; Baschiera, B.; Bihl, M.; Grilli, B.; Herzog, M.; Rebetez, J.; Bubendorf, L. Detection of ROS1-positive non-small cell lung cancer on cytological specimens using immunocytochemistry. *Cancer Cytopathol.* **2018**, 126, 421-429, doi:10.1002/cncy.21983.
45. Nakra, T.; Nambirajan, A.; Guleria, P.; Phulware, R.H.; Jain, D. Insulinoma-associated protein 1 is a robust nuclear immunostain for the diagnosis of small cell lung carcinoma in cytology smears. *Cancer Cytopathol.* **2019**, 127, 539-548, doi:10.1002/cncy.22164.
46. Jain, D.; Nambirajan, A.; Borczuk, A.; Chen, G.; Minami, Y.; Moreira, A.L.; Motoi, N.; Papotti, M.; Rekhtman, N.; Russell, P.A.; Prince, S.S.; Yatabe, Y.; Bubendorf, L. Immunocytochemistry for predictive biomarker testing in lung cancer cytology. *Cancer Cytopathol.* **2019**, 127, 325-339, doi:10.1002/cncy.22137.
47. Metovic, J.; Righi, L.; Delsedime, L.; Volante, M.; Papotti, M. Role of Immunocytochemistry in the Cytological Diagnosis of Pulmonary Tumors. *Acta Cytol.* **2020**, 64, 16-29, doi:10.1159/000496030.
48. Tone, K.; Ohno, S.; Honda, M.; Notsu, A.; Sasaki, K.; Sugino, T. Application of enhancer of zeste homolog 2 immunocytochemistry to bile cytology [published online ahead of print March 31, 2021]. *Cancer Cytopathol.* **2021**, doi:10.1002/cncy.22426.
49. Kujan, O.; Huang, G.; Ravindran, A.; Vijayan, M.; Farah, C.S. CDK4, CDK6, cyclin D1 and Notch1 immunocytochemical expression of oral brush liquid-based cytology for the diagnosis of oral leukoplakia and oral cancer. *J. Oral Pathol. Med.* **2019**, 48, 566-573, doi: 10.1111/jop.12902.